NASA Technical Memorandum 83662

NASA-TM-83662 19840019885

Test Results for 27.5- to 30-GHz Communications Satellite Receivers

Martin J. Conroy
Lewis Research Center
Cleveland, Ohio

June 1984

NASA

Trade names or manufacturers' names are used in this report for identification only. This usage does not constitute an official endorsement, either expressed or implied, by the National Aeronautics and Space Administration.

TEST RESULTS FOR 27.5- TO 30-GHz COMMUNICATIONS SATELLITE RECEIVERS

Martin J. Conroy
National Aeronautics and Space Administration
Lewis Research Center
Cleveland, Ohio 44135

SUMMARY

Tests were performed on five proof-of-concept receivers that had been developed by two contractors, LNR Communications, Inc., and ITT Defense Communications, under the NASA 30/20 GHz Technology Development Program. The receivers operate in the 27.5- to 30-GHz uplink band for communications satellites and produce an output at C band. Receiver requirements and test results are given. Test methods are discussed and results are compared with the contractors' test results.

INTRODUCTION

Studies of the growth in communications traffic indicate that the frequency spectrum allocated to fixed-service satellites at the C and Ku bands will reach saturation by the early 1990's. The next higher frequency bands allocated for communications satellites are 27.5 to 30 GHz for the uplink and 17.7 to 20.2 GHz for the downlink. Current plans for developing satellite systems that use these bands include a NASA demonstration satellite. One of the components that has been identified as critical to the success of that mission is a 27.5- to 30-GHz satellite receiver. Two parallel contracts were let in 1980 to develop proof-of-concept (POC) models of such receivers. In December 1982 the POC models were subjected to a series of tests at Lewis. This report gives the results of these tests and compares them with the results of similar tests performed by the contractors. Table I lists the performance requirements for the receivers. The input radiofrequency band is established by international agreement. The output intermediate frequency (IF) band was specified as 3 to 8 GHz. This allowed the contractors to apply the results of their design studies to receiver designs that would have optimum performance. The other requirements were established by estimating the performance attainable by state-of-the-art techniques without imposing restrictive specifications on one variable at the expense of another. The receivers are shown in figures 1 and 2 and block diagrams in figures 3 and 4.

Both receivers use image-enhanced mixers as the input stage. In these circuits the image frequency band is terminated in a reactance that reflects the power at the image frequency band to the IF band. This provides an improvement in signal strength at no increase in noise level. The first stage of the IF amplifier has a low noise figure, approximately 1.1 dB, and makes a small contribution to the receiver noise figure.

The LNR receivers use a 500-MHz crystal oscillator as the driver for the phase-locked-receiver local oscillator. The 500-MHz signal is multiplied to 23.8 GHz by a step recovery diode. The crystal oscillator, located in the dc-dc converter box, provides sufficient signal level to drive the local

oscillator (LO) multipliers at the three LNR receivers simulataneously. When one receiver is in operation, the unused ports of the power divider are terminated in 50 ohms. The ITT receiver uses a times-three and a times-five multiplier to produce a 25.2-GHz LO signal for the receiver mixer. The reference input for the LO multiplier chain is provided by a Hewlett Packard 8614B Klystron oscillator. A synthesized signal generator is not recommended for this purpose because the generator phase noise modulates the input radio-frequency signal. Each receiver design is described in detail in the respective contractor reports (refs. 1 and 2).

The following tests were performed on each receiver: gain, noise figure, 1-dB compression point, third-order intermodulation, image rejection, AM-PM conversion, group delay, gain slope, input voltage standing-wave ratio (VSWR), output VSWR, dc power, and output spectrum. The measurement techniques and methods were similar to those used by the contractors. Results of the tests are in close agreement with the manufacturers' test results.

GAIN AND NOISE FIGURE

The gain and the noise figure of the LNR receivers were measured with the equipment configured as shown in figure 5. Because the output frequency band of the receivers (3.7 to 6.2 GHz) is greater than the maximum input frequency (1.5 GHz) of the noise figure meter, an external downconverter was used. The downconverter configuration complied with the recommendations in the noise figure meter manufacturer's application note (ref. 3). The downconverter local oscillator was stepped from 2.4 to 4.9 GHz in order to provide a 1.3-GHz input frequency to the noise figure meter. The downconverter local oscillator and the noise figure meter were controlled by a Hewlett-Packard 9845 desktop computer.

The gain and the noise figure of the ITT receivers were measured with the same equipment configuration used for the LNR receivers except that a cavity-tuned signal generator was added to perform the local oscillator driver function for the receiver.

Both solid-state and gas-discharge noise sources are available in the 26.5- to 40-GHz band. Solid-state noise sources with built-in attenuators provide an excess noise ratio (ENR) that is the same as the ENR for gas tubes. However, the variation in ENR in the gas tube over the waveguide band is three times better than the ENR variation of the solid-state sources. The gas-tube standing wave ratio is specified when the discharge occurs and when the discharge is extinguished. Similar standing wave ratio information was not available for the solid-state noise source. For these reasons the gas-discharge noise source was selected for the noise figure tests.

The noise figure meter and the downconverter were calibrated by feeding a noise signal from an Hewlett Packard 346 noise source to the input of the downconverter mixer. Twenty values of ENR that were provided by the noise source manufacturer were set into the noise figure meter. This procedure calibrated the system except for the 30-GHz gas-tube noise source. The gas-discharge noise source and the receiver were then connected to the downconverter mixer, and the single ENR value of the gas-discharge noise source was set into the

noise figure meter. When measurements were made with this method, the uncertainty was due to the combination of the gas-tube ENR uncertainty (±0.5 dB) and the noise figure meter uncertainty (±0.1 dB). The worst-case uncertainty was then ±0.6 dB, or, if root-sum-square is used, ±0.51 dB. Also, the calibration of the gas-tube ENR is given by the manufacturer and not the National Bureau of Standards because the NBS does not provide a noise calibration service in the 27.5- to 30-GHz band.

Plots of the gain and the noise figure for LNR receivers are shown in figures 6 to 11. For receiver 1 the notch at 4100 GHz on the gain curve and a corresponding peak on the noise figure curve were attributed by the receiver manufacturer to a spurious resonance in the mixer current-monitoring path. This resonance was corrected by the manufacturer and does not appear in receivers 2 and 3.

Maximum, minimum, median, and variation values for the gain and the noise figure of each receiver are given in table II along with similar measurements made by the contractor. Receiver 3 has the least variation (3.3 dB) in gain within the passband and receiver 2 has the largest variation (4.6 dB). The Lewis-measured gain variations differed from the LNR-measured gain variations by no more than 0.7 dB. The mean gain of the three receivers is 19.95 dB, which should be rounded to 20 dB.

When the minimum noise figure measurements made at Lewis are compared with the minimum noise figure measurements made by LNR, the largest difference is 0.6 dB. This is within the uncertainty given above. When similar comparisons are made in the maximum noise figure, receivers 1 and 3 fall within the ±0.51 dB rss uncertainty. The maximum noise figure difference for receiver 2 is greater than the worst-case uncertainty.

Spectra of the receiver output show a number of spurious responses in the receiver passband. The noise figure measurements were made in the frequency slots between the spurious responses, and thus the noise figure values were not affected by these responses. Greater detail on these spurious responses is given in the section OUTPUT SPECTRUM.

The gain and the noise figure for ITT receivers 1 and 2 are shown in figures 12 to 15. The the measurements taken at Lewis are compared in table III with the measurements performed at ITT. All measurements agree within 0.7 dB.

COMPRESSION POINT

Figure 16 is a block diagram of the equipment used for the 1-dB compression point test. The 1-dB compression point was measured at 27.5, 28.75, and 30 GHz for each LNR receiver. The power input to the receiver was set at -15 dBm and the receiver IF power output was recorded. The input power was then increased 5 dB by means of the variable attenuator. The receiver power output was measured and the difference between the two output power measurements was recorded. The process was then repeated in 1-dB increments until the 5-dB change in power input produced an output power change of 4 dB or less. If the 4-dB point was not exactly determined by the measurement procedure, its value was obtained by interpolating between values immediately above and below the 4-dB change.

Table IV shows the 1-dB compression points for the three LNR receivers. All of the measurements are greater than 10 dBm. The measurements made at Lewis are in close agreement with the manufacturer's measurements.

The same equipment configuration and procedure were used in an attempt to measure the 1-dB compression point of the ITT receivers. The measurements show that the receivers are linear up to the 10-dBm output level and that the 1-dB compression point could not be reached at signal input levels that would not damage the receivers. These measurements were made at the center of the band, 28.75 GHz. The results agree with those reported by ITT.

Curves of power output versus power input for all of the receivers are shown in figures 17 and 18. The tests were performed at the center frequency of the uplink band (28.75 GHz).

THIRD-ORDER INTERMODULATION

The equipment used for measuring the third-order intermodulation products is shown in figure 19. The test specification was that two equal signals of -30 dBm at the receiver input, separated by 0.2 GHz or less, should produce third-order intermodulation products that are more than 50 dB below the carrier.

Figure 20 shows the results of the intermodulation test on LNR receiver 1. The two input signals translated to IF are shown at 4.728 and 4.9 GHz. The signal input level (-30 dBm) is less than the level shown in the figure by the gain of the receiver (20 dB). The spurious responses of the LNR receiver can obscure the intermodulation products. To identify the products, one of the -30-dBm input signals was switched on and off. The product at 4.556 GHz is identified by the spectrum analyzer marker at -72.5 dBm. The second intermodulation product is shown at 5.072 GHz, -72.5 dBm. The other responses are receiver spurious responses. Figures 21 and 22 give similar information on receivers 2 and 3.

The results of the intermodulation product test on the ITT receives are shown in figures 23 and 24 and summarized in table V.

IMAGE RESPONSE

The equipment setup for the image response test is shown in figure 25. The receiver performance requirement for image rejection is a minimum of 15 dB. The image frequency band is 20.4 to 22.9 GHz for the ITT receiver and 17.6 to 20.1 GHz for the LNR receiver. The frequency selected for the image rejection test at Lewis was at the high end of the image passband. Slight adjustments were made to the LNR image test frequency to assure that the image response would fall between the receiver spurious responses. Figure 26 shows the output response of LNR receiver 1. The marker has been placed on the image response. The input signal of -20 dBm at 20.1 GHz produced an image response that was 64 dB below the input signal. The other two LNR receivers (figs. 27 and 28) produced no image responses that were visible above the noise level of the spectrum analyzer.

Figures 29 and 30 show the results of the image response test on the ITT receivers. The response that is identified by the spectrum analyzer marker was caused by a -20-dBm signal at 22.9 GHz. The response is more than 50 dB below the input signal. The results of the image response test are summarized in table VI.

The signals at 5.1 GHz in both ITT receivers are spurious responses, but they fall outside the IF passband. ITT receiver 2 shows a spurious response at 4.65 GHz with an amplitude of -82 dBm. The source of this signal has not been identified.

AMPLITUDE MODULATION - PULSE MODULATION CONVERSION

The AM-PM requirement for the receivers was less than 1 deg/dB for input carriers of signal level no greater than -70 dBm. The technique used to make the measurements was adapted from a technique used to measure the AM-PM conversion of traveling-wave tubes (ref. 4). The block diagram of the instrumentation is identical to that used for the third-order intermodulation tests (fig. 19). In these tests the input signals were of equal amplitude. In the AM-PM tests the input signals differed in amplitude by 30 dB. The radiofrequencies of the two generators were nominally 28.5 and 28.7 GHz. The actual radiofrequencies were set to values that would avoid coincidence with the spurious output responses of the LNR receivers, would occupy a portion of the passband that had an amplitude variation of less than 1 dB, and would be close to the center of the passband.

From the difference between the two large responses and the difference between the largest response and the third-order intermodulation product (as displayed on a spectrum analyzer), the AM-PM conversion factor was calculated by using equation (1). The equation was modified from reference 5 to yield the AM-PM conversion factor, in units of degrees per decibel, for the case where the two input signals differ by 30 dB.

$$K_p = 13.2 \left[S_1^2 - \left(\frac{1 + S_1^2 - S_2^2}{2} \right)^2 \right]^{1/2} \qquad (1)$$

where

$$S_1 = 10 \left(\frac{30 - \Delta_1}{20} \right)$$

$$S_2 = 10 \left(\frac{30 - \Delta_2}{20} \right)$$

and

Δ_1 difference in decibels between the two carriers

Δ_2 difference in decibels between the larger carrier and the third-order intermodulation product

The results are shown in table VII. The measured values of AM-PM conversion are within the original requirements.

The measurements were made at a signal input level of -15 dBm. This was 55 dB above the required level. The measurements were not made at -70 dBm because the responses to the input signals would have been well below the noise level of the spectrum analyzer.

LNR calculated the AM-PM conversion factor by using the third-order intercept point. They obtained AM-PM conversion factors of 0.5 to 0.8 deg/dB, at signal input of -15 dbm. These values were within the original requirements. ITT measured the receiver response to the two-signal input and calculated the AM-PM conversion factor. Their results were less than 0.1 deg/dB and are comparable to the results obtained at Lewis. (Measurements were not made on LNR receiver 2 because of an equipment failure.)

GROUP DELAY

A block diagram of the group delay measurement method is shown in figure 31. The measurement technique and derivation are given in reference 5. Before the test a phase zero for the vector voltmeter was obtained by placing a waveguide crystal detector at the output of the waveguide that feeds the receiver. The crystal detector output was fed to channel B of the vector voltmeter and compared with the pin diode modulating reference signal. The receiver and the 8473C detector were then inserted in place of the waveguide crystal detector. The radiofrequency signal was swept from below 27.5 to above 30 GHz. The group delays for the five receivers are shown in figures 32 to 36.

Perturbations in the group delay curves correspond to variations in the amplitude characteristics. This is evident when the group delay curve for LNR receiver 1 is compared with the gain and noise figure curves for LNR receiver 1 between 27.5 and 28 GHz. At this frequency range resonance occurred in the mixer current monitoring path. Excluding this point, the maximum group delay ripple from peak to adjacent peak for each group delay curve is given in table VIII. The receivers meet the 5-ns group delay ripple requirement.

Neither manufacturer measured the group delay of their receivers. LNR calculated the group delay ripple by approximating the amplitude response of the IF amplifier with a 5-pole Chebychev filter. The calculated ripple of this approximation was 0.346 ns, which is about one-third of the measured value for LNR receiver 1.

GAIN SLOPE

The gain-slope requirement for the receivers was ±0.5 dB per 10 MHz. To test the LNR receivers for this requirement, a leveled -23-dBm sweep was fed to the receivers, and spectrum analyzer plots of the receiver IF output were made (figs. 37 to 39). For LNR receiver 1 the positive and negative slopes of the large notch at 4.095 GHz and the positive slope at 6.065 GHz were calculated.

For LNR receivers 2 and 3, only the large negative slopes near the center of the band were calculated.

For the ITT receivers the plots of gain versus frequency previously obtained for the gain and noise figure measurements were inspected and the portion of the curve with the largest slope was selected. From the tabular data for the gain curves the gain slope was calculated. The three slopes for LNR receiver 1 and one slope for each of the other receivers are given in table IX. All of the receivers except LNR receiver 1 meet the requirement. This receiver meets the requirement if the large notches at 4 and 6 GHz are neglected.

INPUT VOLTAGE STANDING-WAVE RATIO

The equipment configuration that was used for measuring the VSWR of the radiofrequency input port for the ITT receivers is shown in figure 40. The configuration uses a spectrum analyzer as the reflected-power indicator because it can be used to measure the reflected power in the receiver passband and to disregard the receiver local oscillator feedthrough signal. For the ITT receivers the receiver local oscillator signal at the radiofrequency input port was -26 dBm at 25.2 GHz. The input VSWR measurement results are given in table XI for both ITT receivers, and the results are plotted and compared with the manufacturers' data in figures 41 and 42. Although two different methods were used to measure the input standing-wave ratio (ITT, slotted line; Lewis, reflectometer), the results are comparable.

The input VSWR of the LNR receiver was measured with the equipment used for the ITT receivers. To reduce the effects of the receiver local oscillator signal on the reflected signal, a waveguide-below-cutoff filter was inserted at the output of the reflected signal coupler. This reduced the local oscillator signal at the output of the coupler from -15 dBm to less than -65 dBm. The results of the input VSWR measurements on the receivers are plotted in figure 43. The envelope of input VSWR measurements made by the contractor is shown by the dashed line.

OUTPUT VOLTAGE STANDING-WAVE RATIO

The output VSWR of each of the receivers was measured by an automatic vector network analyzer (ANA). These plots are shown in figures 44 to 48. The values of output VSWR reported by the manufacturers are shown as circled points. LNR reported three measurements of output VSWR for each receiver: one at the lower end of the passband, another at the high end of the passband, and a maximum value measured at an unspecified frequency within the passband. The VSWR's at the higher and lower frequencies are plotted on the corresponding Lewis-generated curve. Both LNR and Lewis measurements fall within the 1.8:1 output VSWR requirement.

ITT measured the output VSWR on an ANA. A few points from their curves are plotted on the Lewis curves for comparison. Both sets of measurements are well below the 1.8:1 VSWR requirement.

DIRECT-CURRENT POWER

LNR provides a dc power conditioner to supply ±15 and ±5 V for operation of the receiver, and to provide power for the 500-MHz receiver crystal oscillator that is located in the power conditioning box. The steady-state current drawn from the 28-V supply is 700 mA for receiver 1,750 mA for receiver 2, and 640 mA for receiver 3. The in-rush current drawn from the 28-V supply for receivers 2 and 3 is approximately 28 A. This transient decays to the steady-state value within 2.5 ms. The 28-V dc power supply must be capable of supply ing the in-rush current. The in-rush current requirement for receiver 1 is 12 A.

ITT supplied its power conditioner with a power-sequencing switch that applies gate bias to the amplifiers before drain voltage is applied. There is no measurable dc turn-on transient in the ITT receivers. The steady-state dc current draw is nominally 225 mA for each receiver.

OUTPUT SPECTRUM

To determine what spurious responses were generated in the receivers, spectrum analyzer plots were obtained at the IF output for each receiver. These plots are shown in figures 49 to 53. In all cases, no radiofrequency signal was fed to the input of the receivers. ITT receiver 1 has two spurious responses. They occur just outside the IF passband (2.3 to 4.8 GHz). The response at 5.04 GHz at -45 dB is due to the third harmonic of the receiver local oscillator input signal. The source of the 2.256-GHz signal was not determined. ITT receiver 2 does not show a response at 2.256 GHz. Note that desired signals at the low end of the IF band, when mixed with the 5.04-GHz spurious response in nonlinear devices following the receiver, will produce intermodulation products within the receiver IF band.

Figures 51 to 53 show the output spectrum of the three LNR receivers when there is no signal present at the input. In receiver 1, spurious responses occur at multiples of 500 MHz. This is the frequency of the crystal oscillator whose function is to drive the receiver local-oscillator multiplier chain. Receivers 2 and 3 show groups of spurious responses that repeat at 500-MHz intervals. Analysis by the manufacturer indicates that the cause of the spurious responses is the local oscillator multiplier for the step recovery diode. The manufacturer applied internal shields to receiver 1, but not to receivers 2 and 3. The reduction in the number of spurious responses clustered around the 500-MHz multiples is evident when either receiver 2 or 3 is compared with receiver 1.

The frequency and level of the spurious responses were determined by using the spectrum analyzer marker and are shown directly on LNR receiver 1 output spectrum (fig. 51).

The amplitude and frequency of each spurious response in receiver 3 are given in table XI. Similar data for receiver 2 can be obtained from the output spectrum plot (fig. 52).

CONCLUSIONS

The receivers supplied by both contractors met most of the requirements. Both contractors approached the noise figure requirement of 5 dB near the midpoint of the receiver passband, but the noise figure increased by 3 to 5 dB at the high and low ends of the passband. This increase should be considered when communications bands and center frequencies are assigned. Receiver gain also varied in the passband and must be considered in frequency band assignments.

The LNR receivers had a set of spurious responses within the receiver passband. Use of the receivers to their maximum dynamic range will be restricted to the spaces between the spurious responses.

All of the receivers have met the intent of the proof-of-concept contracts.

REFERENCES

1. Steffek, L. J.; and Smith, D. W.: The 30 GHz Communications Satellite Low Noise Receiver. (LNR-400, LNR Communications, Inc.; NAS3-22494.) NASA CR-168254, 1983.

2. ITT Defense Communications: 30/20 GHz Communications Satellite Low Noise Receiver. NASA CR-168184, 1983.

3. Applications and Operation of the 8970A Noise Figure Meter. Product Note 8970A-1, Hewlett Packard, 1982.

4. Laico, J.P.; McDowell, H. L.; and Moster, C. R.: A Medium Power Traveling-Wave Tube for 6,000-Mc Radio Relay. Bell Syst. Tech. J., vol. 35., Nov. 1956, pp. 1285-1346.

5. Swept-Frequency Group Delay Measurements. Application Note, Hewlett Packard, 1968.

TABLE I. - PERFORMANCE REQUIREMENTS

Input radiofrequency band, GHz	27.5 to 30
Output intermediate frequency, GHz	3 to 8
Noise figure, dB	5
Radio- to intermediate-frequency gain, dB	20
In-band overdrive for no permanent degradation, dBm	-10
Gain variation, dB	±1
Gain slope, dB per 10 MHz	±0.5
Voltage standing-wave ratio (VSWR) input (max.)	1.25
Voltage standing-wave ratio (VSWR) output (max.)	1.8
Group delay:	
Parabolic, ns/mHz$_2$/100 MHz	±0.1
Ripple, ns p-p (max.)	5
Image rejection, at IF output, dB	15
AM-PM conversion for input carriers up to -70 dBm, deg/dB	1
dc power (±10 percent), V dc	28
Connectors:	
Input	WR 28
Other[a]	SMA
dc	Optional

[a]Radio/intermediate frequency.

TABLE II. - LEWIS AND LNR MEASUREMENTS OF GAIN AND NOISE FIGURE

	Lewis measurement, dB	LNR measurement, dB
Gain		
Receiver:		
Maximum gain	21.8	21.8
Minimum gain	18.0	18.7
Median	19.9	20.25
Passband variation	3.8	3.1
Receiver 2:		
Maximum gain	21.6	21.8
Minimum gain	17.0	16.8
Median	19.3	19.3
Passband variation	4.6	5.0
Receiver 3:		
Maximum gain	22.3	21.8
Minimum gain	19.0	18.8
Median	20.65	20.3
Passband variation	3.3	3.0
Mean, three receivers	19.95	19.95
Noise figure		
Receiver 1:		
Minimum	5.8	5.2
Maximum	8.5	7.5
Median	7.15	6.35
Variation	2.7	2.3
Receiver 2:		
Minimum	6.3	6.1
Maximum	10.8	9.3
Median	8.55	7.7
Variation	4.5	3.2
Receiver 3:		
Minimum	5.9	5.3
Maximum	8.5	7.5
Median	7.2	6.4
Variation	2.6	2.2
Mean, three receivers	7.6	6.8

TABLE III. - LEWIS AND ITT MEASUREMENTS OF GAIN AND NOISE FIGURE

	Lewis measurement, dB	ITT measurement, dB
Gain		
Receiver 1:		
Maximum	19.8	20.4
Minimum	14.7	15.4
Median	17.3	17.9
Passband variation	5.1	5.0
Receiver 2:		
Maximum	19.3	19.3
Minimum	14.5	15.0
Median	16.9	17.2
Passband variation	4.8	4.3
Noise figure		
Receiver 1:		
Maximum	9.9	9.4
Minimum	6.1	5.4
Median	8.0	7.4
Passband variation	3.8	4.0
Receiver 2:		
Maximum	9.2	8.95
Minimum	6.8	6.2
Median	8.0	7.55
Passband variation	2.4	2.75

TABLE IV. - 1-dB COMPRESSION POINT OF LNR RECEIVERS

Receiver	Frequency, GHz	1-dB Compression point, dBm	
		Manufacturer	Lewis
1	27.5	+12.8	12.7
	28.75	+13.5	13.1
	30.0	+12.9	13.0
2	27.5	+12.2	13
	28.75	+11.8	13.1
	30.0	+11.8	12.7
3	27.5	+12	11.6
	28.75	+11.8	12.5
	30.0	+11.6	12.7

TABLE V. - INTERMODULATION PRODUCT SUMMARY

Receiver	Median output signal level, dBm	Median intermodulation level, dBm	Level difference, dB
LNR 1	-10.9	-72.5	61.6
LNR 2	-12.5	-73.4	60.9
LNR 3	-10.5	-71.3	60.9
ITT 1	-11	-75.5	64.5
ITT 2	-12	-74	62.0

TABLE VI. - IMAGE RESPONSE SUMMARY

Receiver	Input		Output		Response, dB
	Frequency, GHz	Level, GHz	Frequency, GHz	Level, dBm	
LNR 1	20.1	-20	3.7	-84	64
LNR 2	20.1	↓	3.7	<-85	>65
LNR 3	20.1	↓	3.7	<-85	>65
ITT 1	22.9	↓	2.3	-75	55
ITT 2	22.9	↓	2.3	-77	57

TABLE VII. - AM-PM
CONVERSION FACTOR

Receiver	AM-PM conversion factor at -15-dBm input power, deg/dB
LNR 1	0.3
LNR 2	----
LNR 3	.5
ITT 1	.19
ITT 2	.15

TABLE VIII. - GROUP DELAY RIPPLE

[Ripple requirements, 5 nsec peak to peak.]

Receiver	Ripple, nsec p-p	Frequency range, GHz
LNR 1	1	29.5-30
LNR 2	4	28.5-29
LNR 3	3	28.5-29
ITT 1	4	29.5-30
ITT 2	4	29.5-30

TABLE IX. - SUMMARY OF GAIN SLOPE MEASUREMENTS

Receiver	Intermediate frequency, GHz	Gain-slope, dB/10 MHz
LNR 1	4.050	-0.485
LNR 1	4.095	.713
LNR 1	6.065	1.097
LNR 2	4.88	-.16
LNR 3	4.69	-.06
ITT 1	2.5	-.2
ITT 2	2.45	-.19

TABLE X. - INPUT VOLTAGE STANDING-WAVE RATIO MEASUREMENTS, ITT RECEIVERS

Frequency, GHz	ITT 1		ITT 2	
	ITT	Lewis	ITT	Lewis
	Input VSWR			
27.5	1.65	1.61	1.55	1.65
28.0	1.85	2.00	1.6	1.92
28.5	1.4	1.61	1.32	1.67
29.0	1.3	1.36	1.27	1.34
29.5	2.4	2.75	2.7	2.58
30.0	3.0	4.53	3.1	3.38

TABLE XI. - SPURIOUS RESPONSES, LNR 3

Intermediate frequency, GHz	Amplitude, dBm	Radio-frequency, GHz	Intermediate frequency, GHz	Amplitude, dBm	Radio-frequency, dBm
2.93	-75.4	26.73	4.43	-71.7	28.23
2.97	-75.6	26.77	4.47	-65.3	28.27
3.00	-65.8	26.8	4.50	-53.0	28.30
3.03	-66.6	26.83	4.53	-56.9	28.33
3.06	-66.0	26.86	4.565	-75.1	28.37
3.09	-75.7	26.89	4.595	-77.9	28.40
3.095	-67.3	26.9	4.9	-79.0	28.70
3.40	-77.7	27.2	4.93	-74.5	28.73
3.43	-73.7	27.23	4.965	-66.7	28.77
3.465	-77.6	27.27	5.00	-68.5	28.80
3.50	-76.0	27.30	5.03	-68.8	28.83
3.53	-72.2	27.33	5.40	-78.8	29.20
3.565	-75.8	27.37	5.43	-74.9	29.23
3.595	-77.6	27.40	5.445	-76.9	29.25
3.93	-78.2	27.73	5.465	-76.3	29.27
3.97	-80.2	27.27	5.50	-79.0	29.30
3.995	-68.2	27.80	5.53	-75.2	29.33
4.03	-66.1	27.83	5.95	-45.9	29.75
4.065	-76.2	27.87	7.38	-62.7	31.18
4.10	-78.3	27.90			

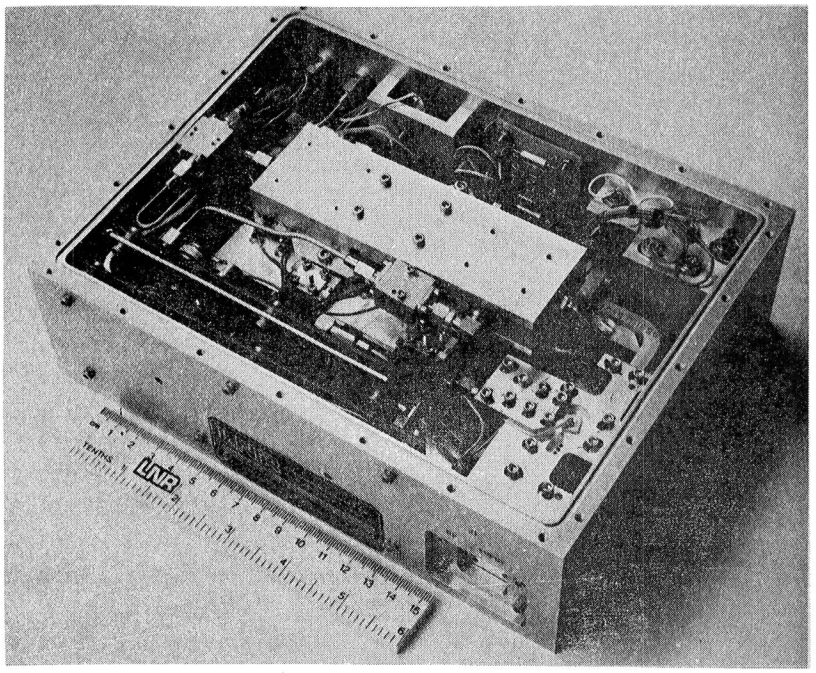

Figure 1. - LNR receiver.

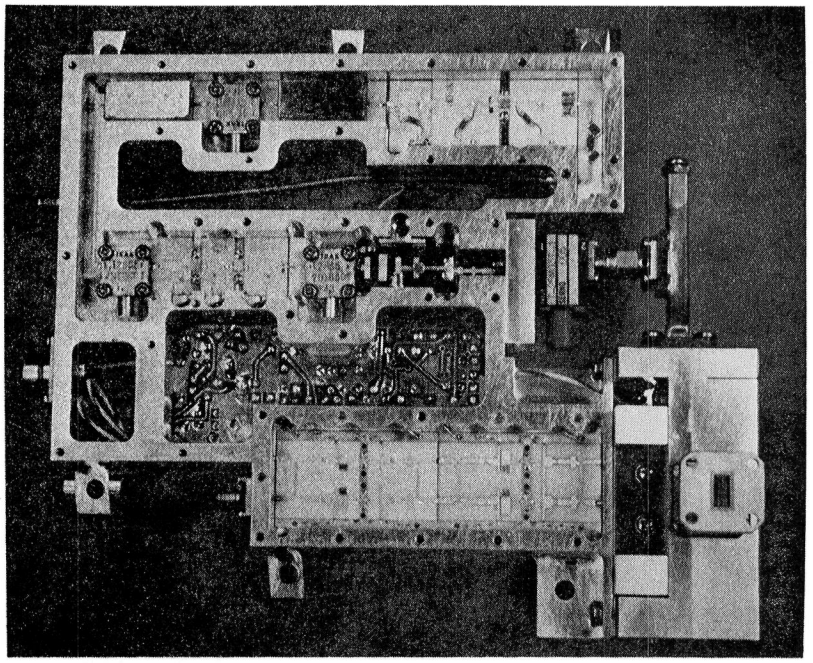

Figure 2. - ITT receiver.

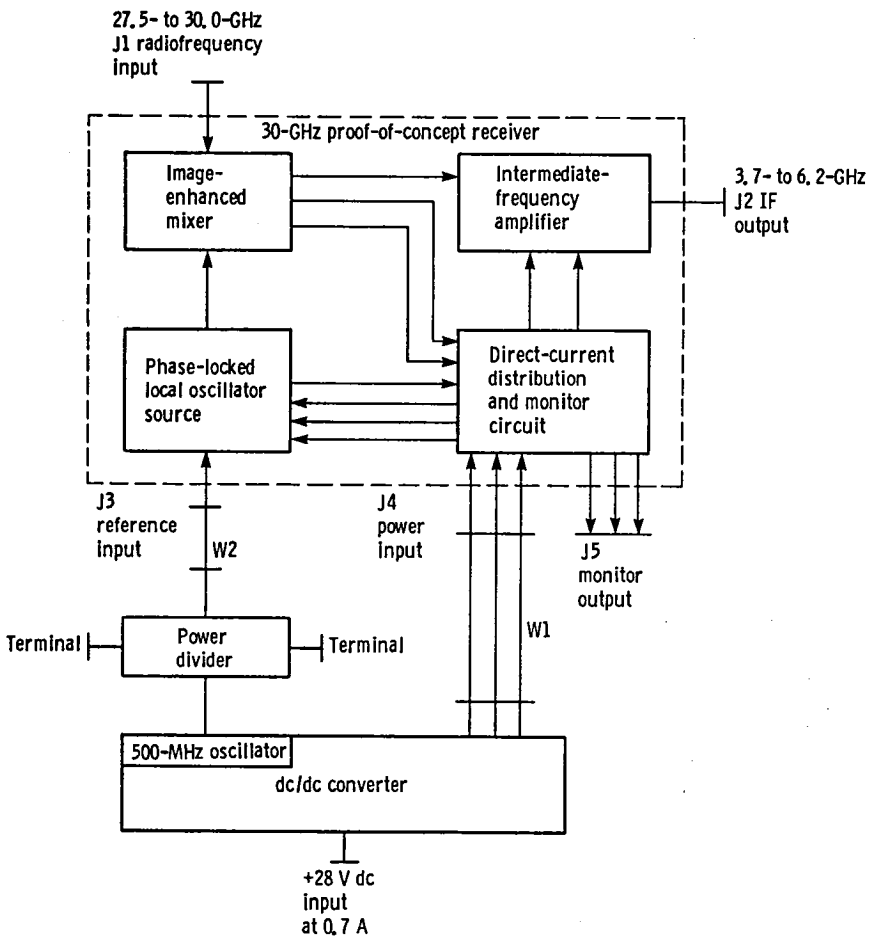

Figure 3. - Block diagram of LNR receiver.

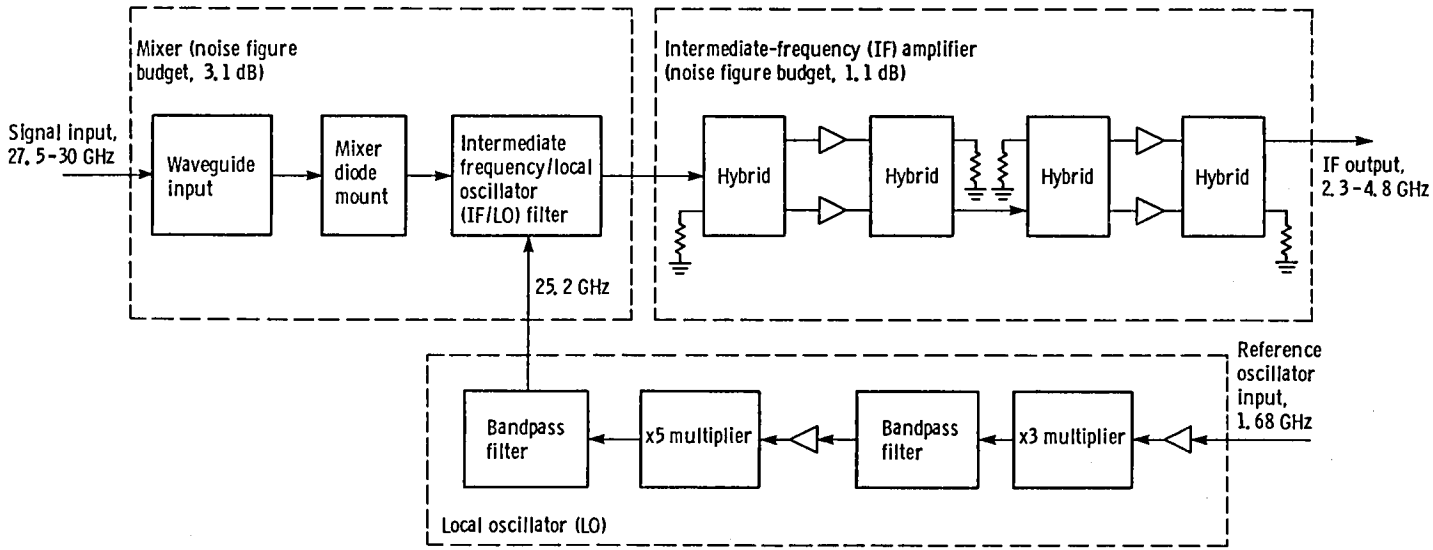

Figure 4. - Block diagram of ITT receiver.

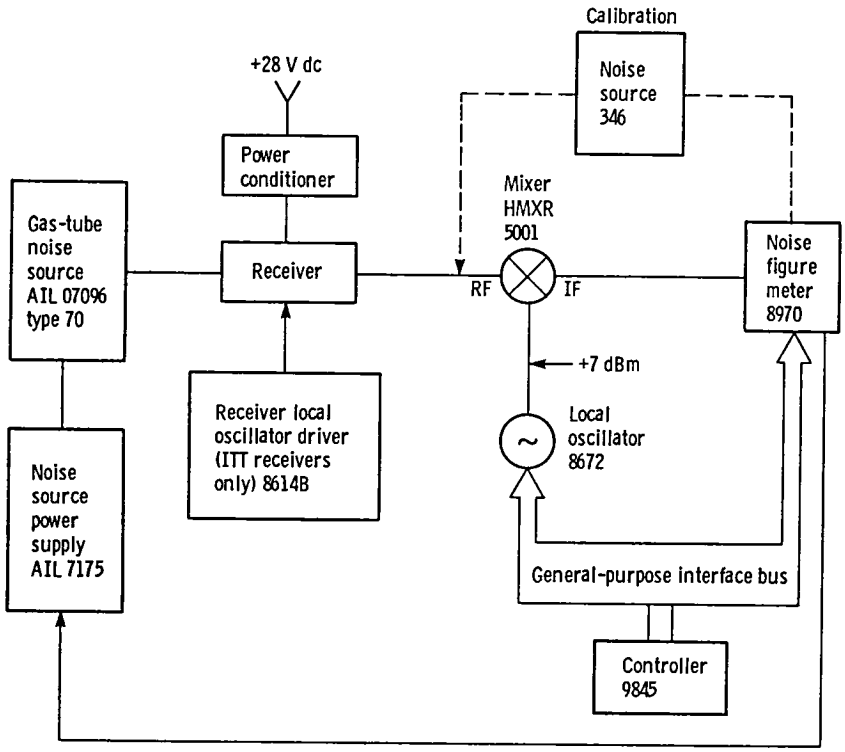

Figure 5. - Block diagram of gain and noise figure tests.

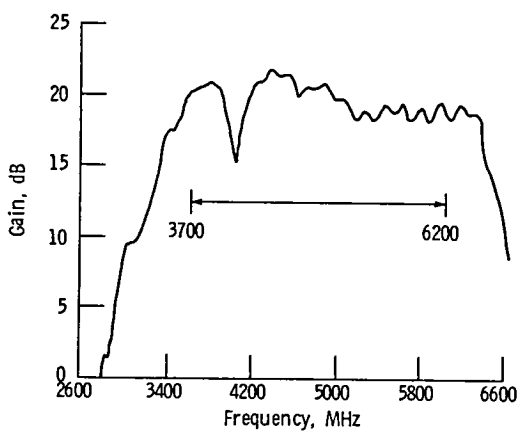

Figure 6. - Gain versus intermediate output frequency, LNR receiver 1.

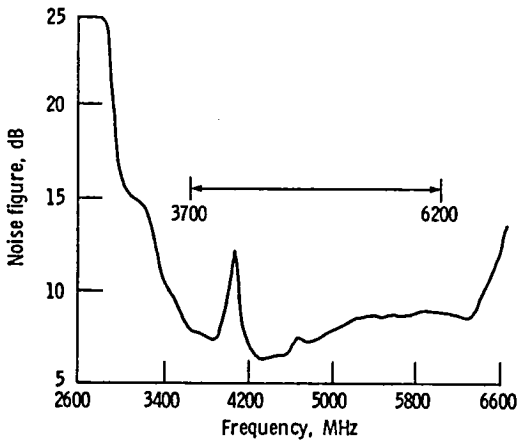

Figure 7. - Noise figure versus intermediate output frequency, LNR receiver 1.

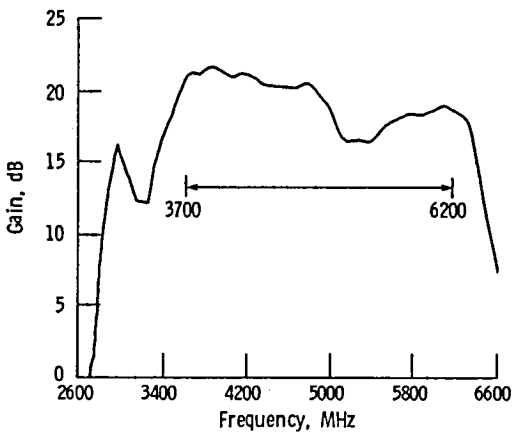

Figure 8. - Gain versus intermediate output frequency, LNR receiver 2.

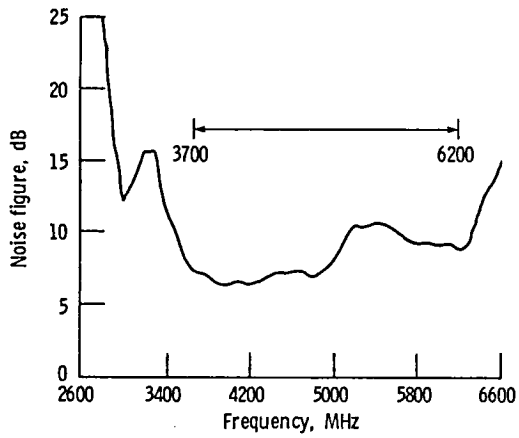

Figure 9. - Noise figure versus intermediate output frequency, LNR receiver 2.

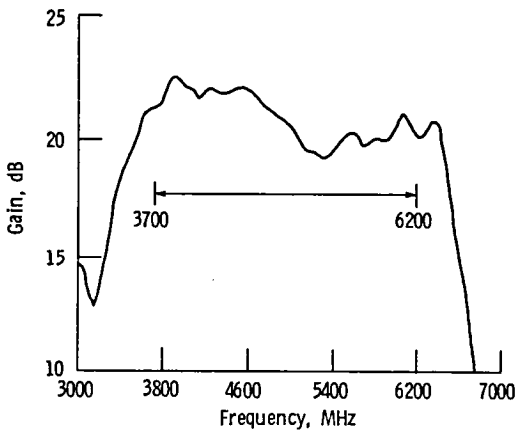

Figure 10. - Gain versus intermediate output frequency, LNR receiver 3.

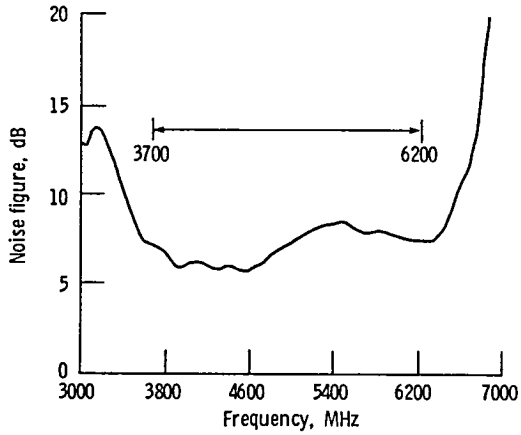

Figure 11. - Noise figure versus intermediate output frequency, LNR receiver 3.

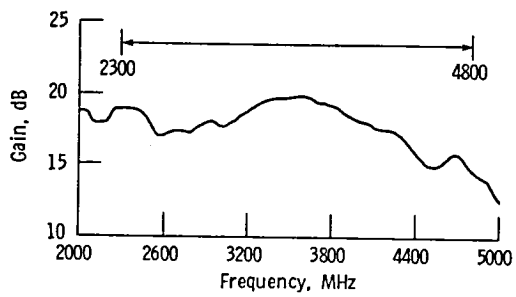

Figure 12. - Gain versus intermediate output frequency, ITT receiver 1.

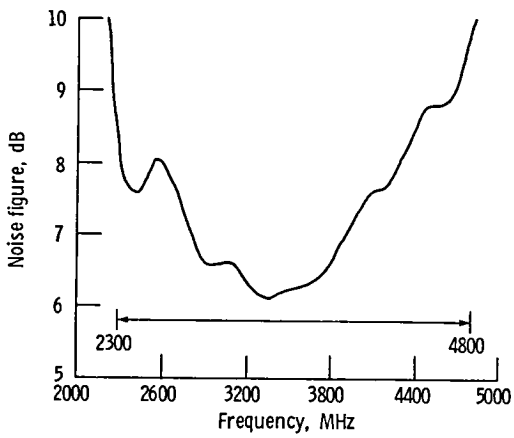

Figure 13. - Noise figure versus intermediate output frequency, ITT receiver 1.

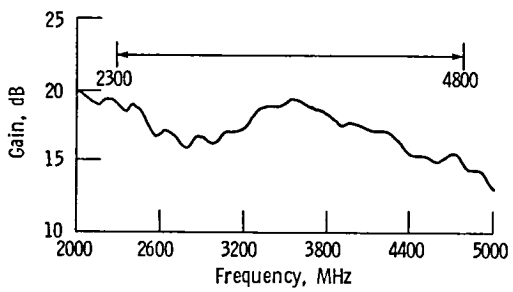

Figure 14. - Gain versus intermediate output frequency, ITT receiver 2.

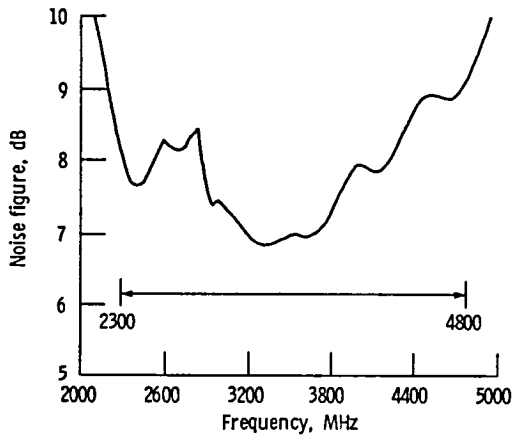

Figure 15. - Noise figure versus intermediate output frequency, ITT receiver 2.

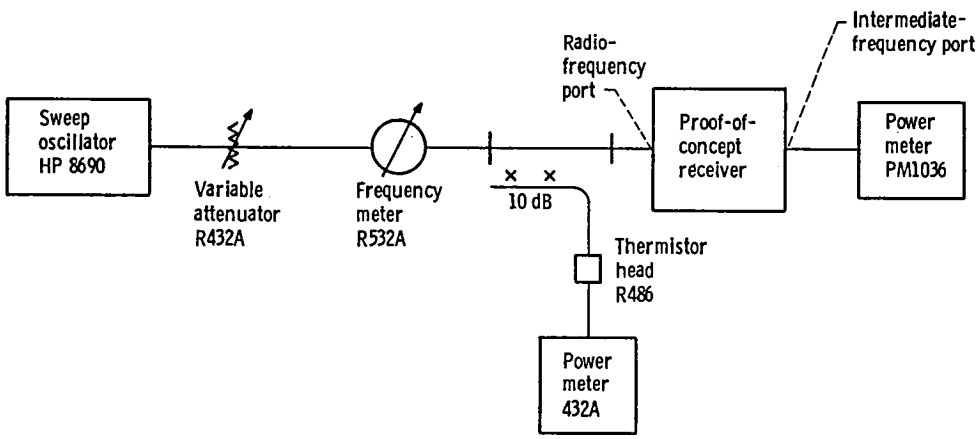

Figure 16. - Block diagram of 1-dB compression point test.

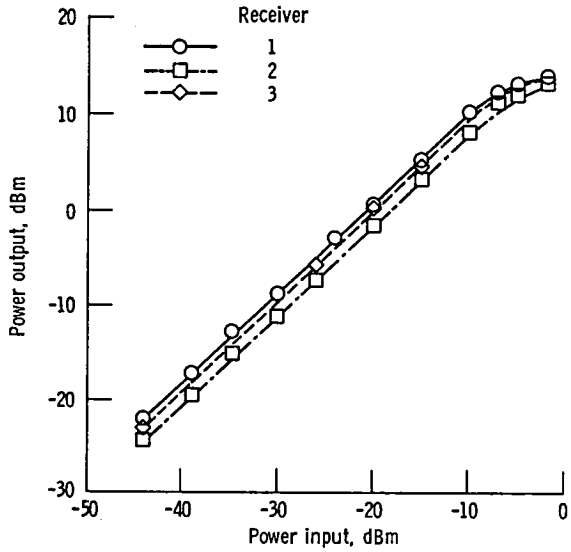

Figure 17. - Power curves for LNR receivers.

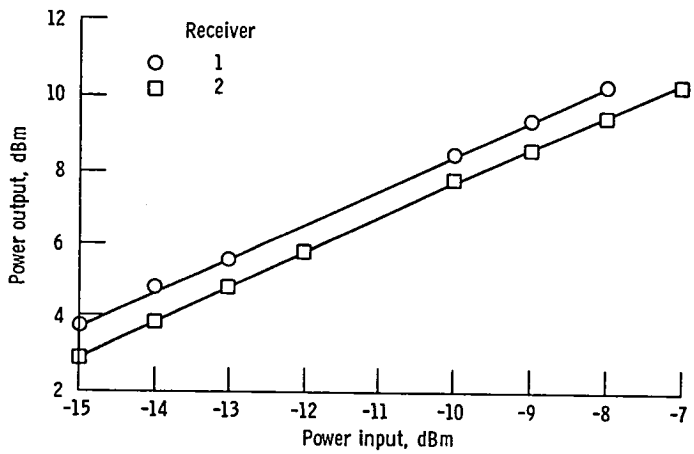

Figure 18. - Power curves for ITT receivers.

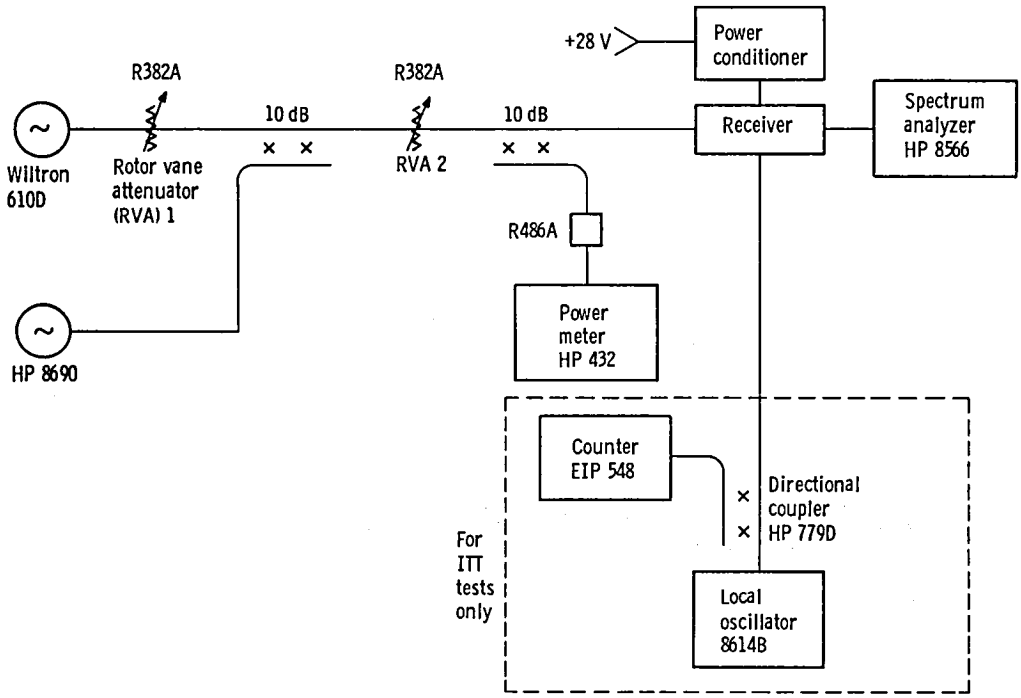

Figure 19. - Block diagram of third-order intermodulation tests, ITT and LNR receivers.

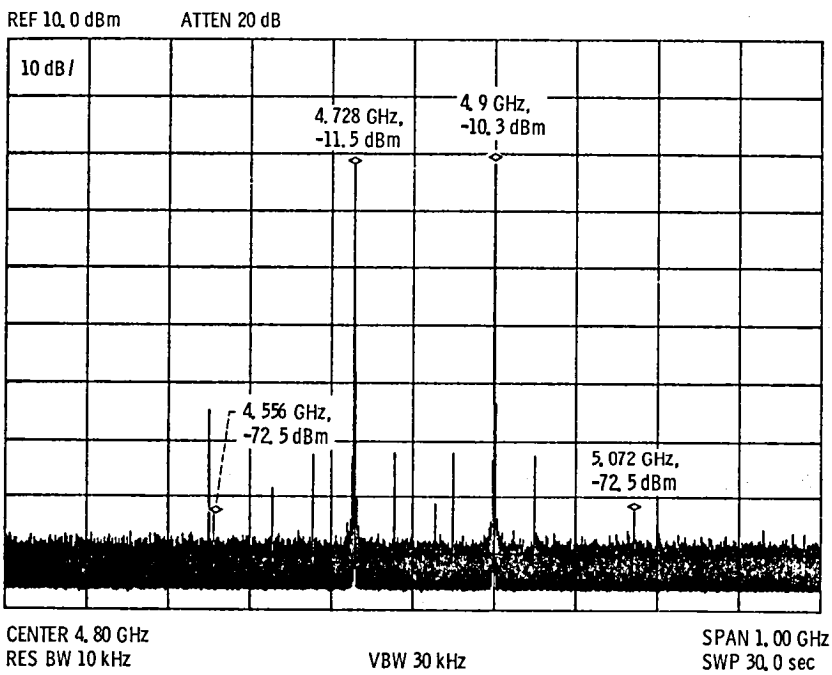

Figure 20. - LNR-1 third-order intermodulation test (7/21/83).

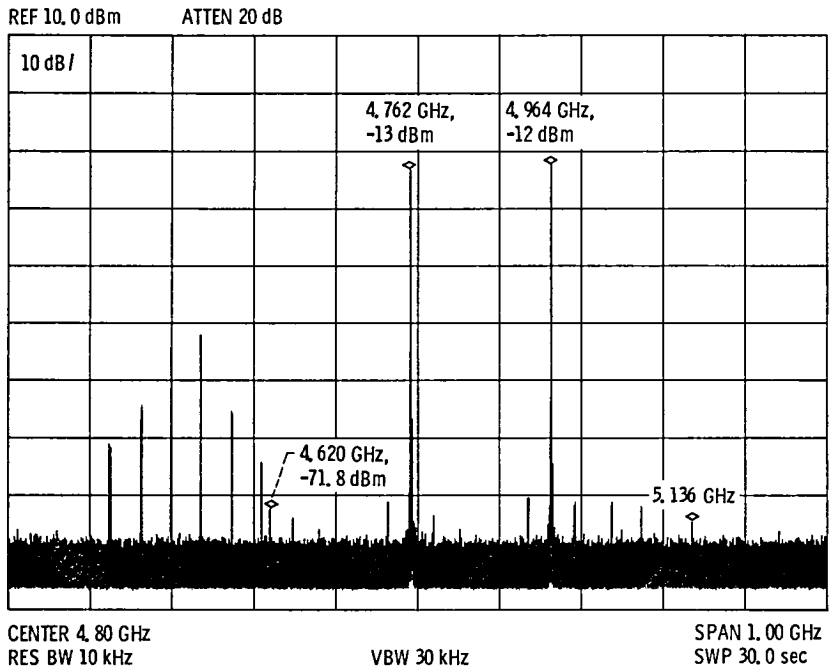

Figure 21. - LNR-2 third-order intermodulation test (6/7/83).

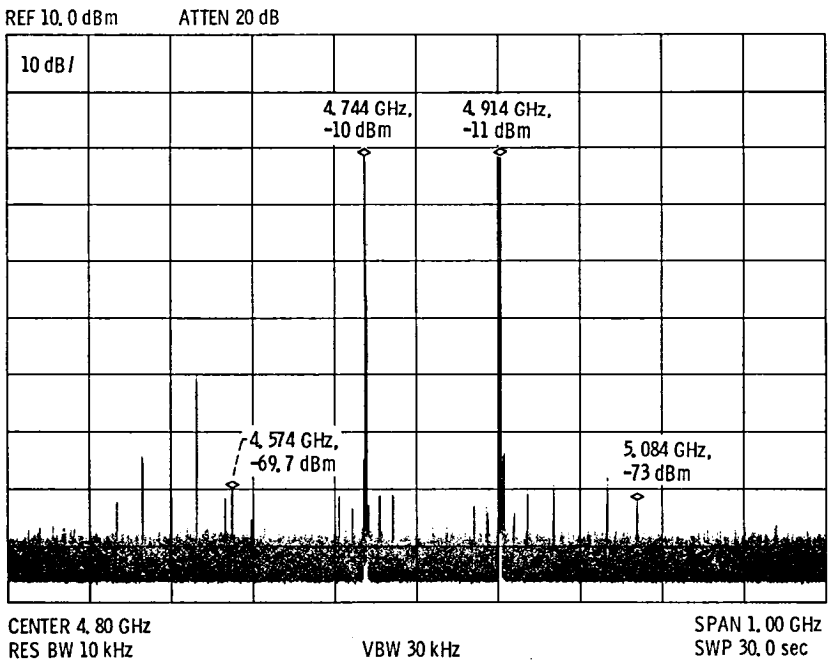

Figure 22. - LNR-3 third-order intermodulation test (6/6/83).

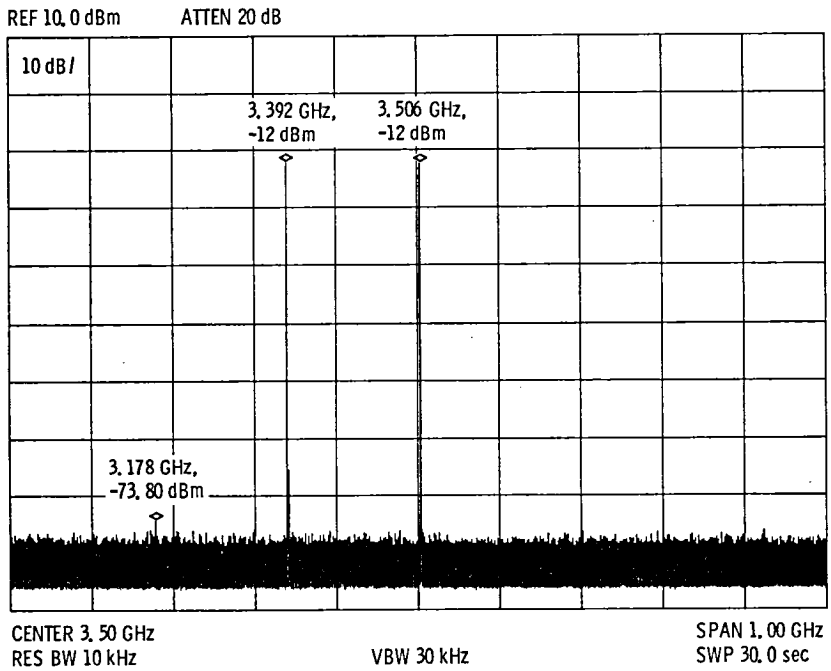

Figure 23. - ITT-1 third-order intermodulation test (6/6/83).

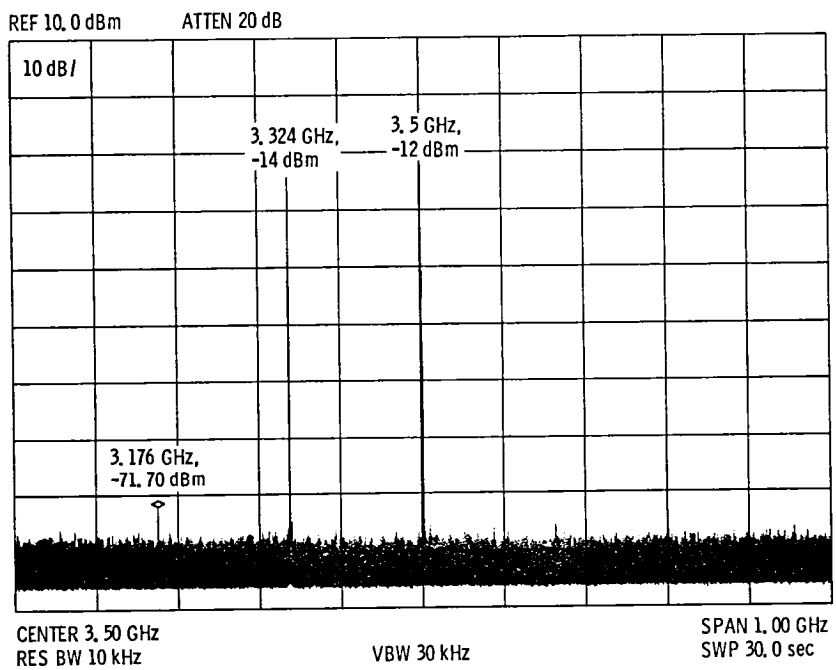

Figure 24. - ITT-2 third-order intermodulation test (6/6/83).

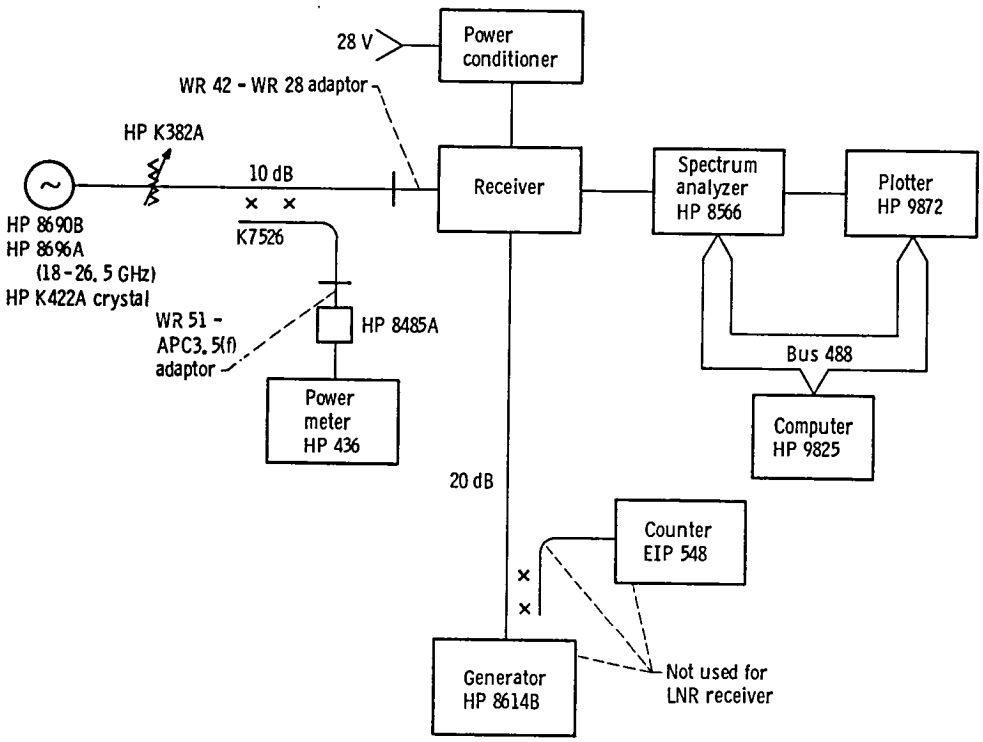

	ITT	LNR
Radiofrequency, GHz	27.5-30	27.5-30
Local oscillator, GHz	25.2	23.8
Intermediate frequency, GHz	2.3-4.8	3.7-6.2
Image, GHz	20.4-22.9	17.6-20.1
Image specification, dBm at receiver output	<-15	<-15

Figure 25. - Equipment configuration for image response tests.

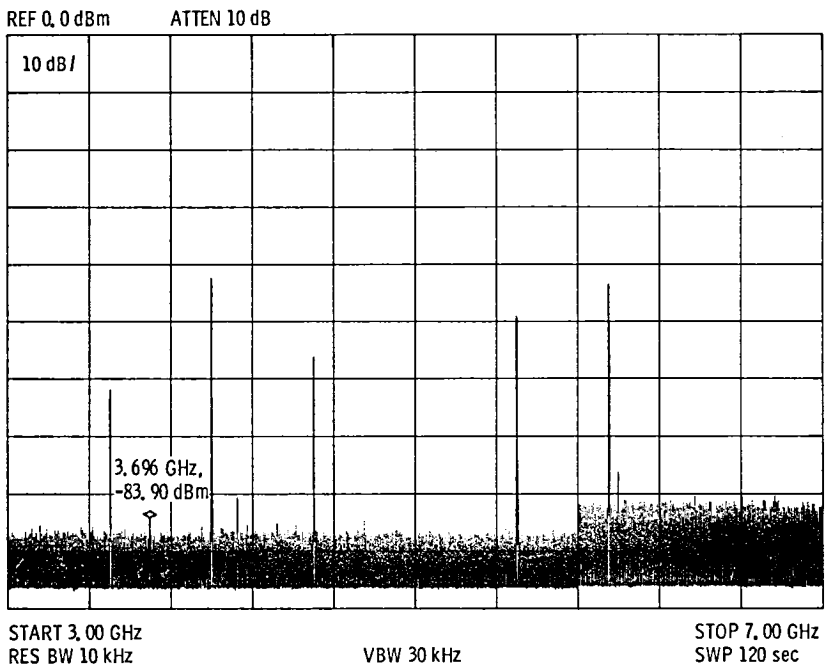

Figure 26. - LNR-1 image rejection test (7/22/83). Input, 20.1 GHz at -20 dBm.

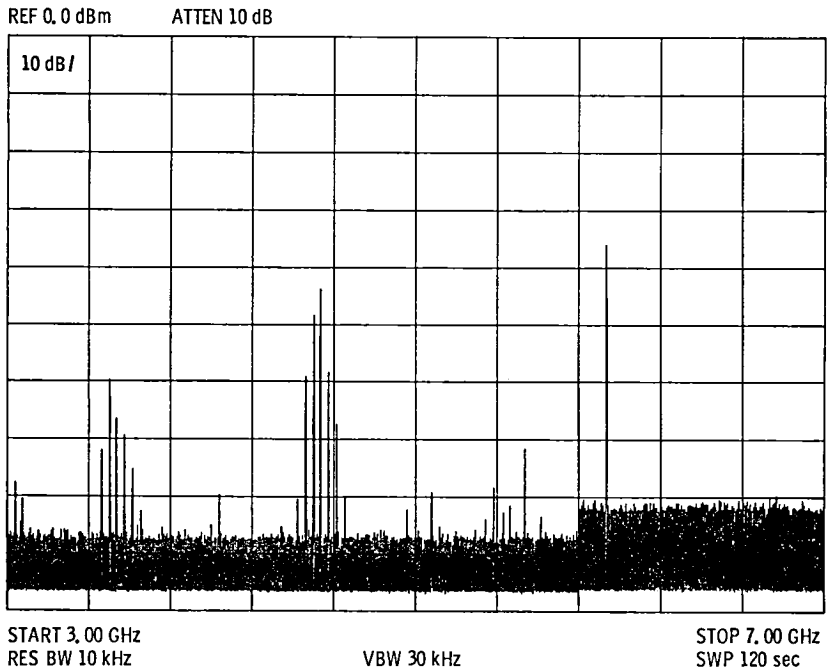

Figure 27. - LNR-2 image rejection test (6/9/83). Input, 20.1 GHz at -20 dBm (no visible image).

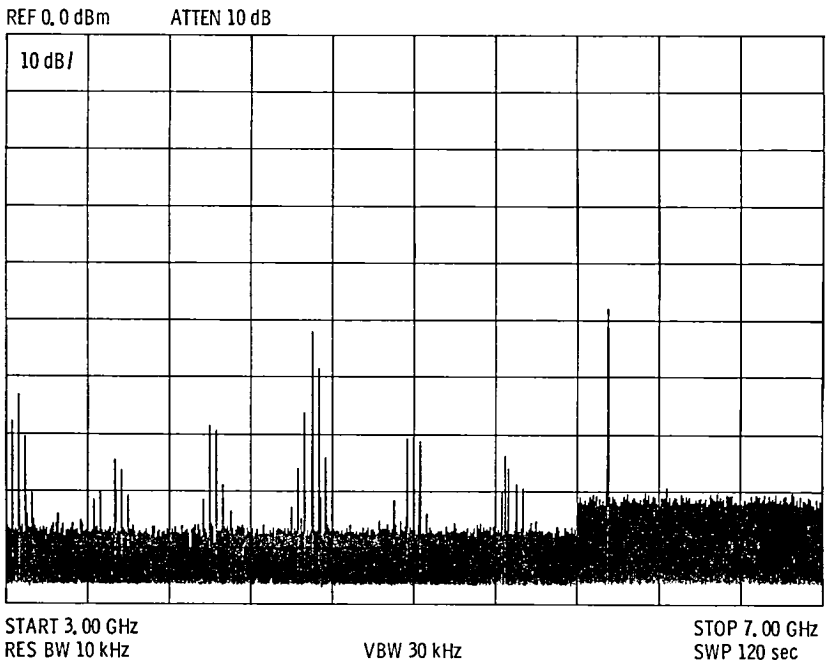

Figure 28. - LNR-3 image rejection test (6/10/83). Input, 20.1 GHz at -20 dBm (no visible image).

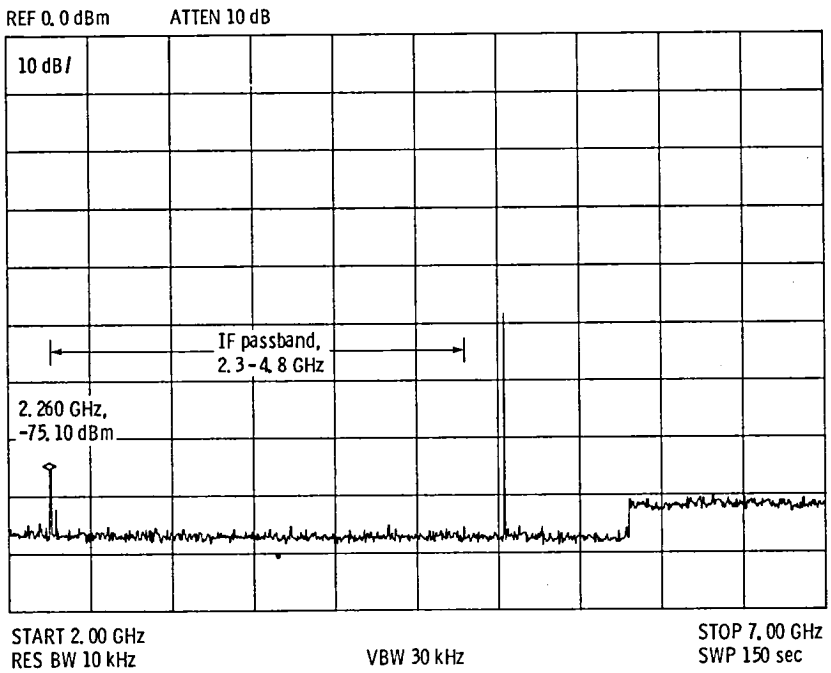

Figure 29. - ITT-1 image rejection test (6/8/83).

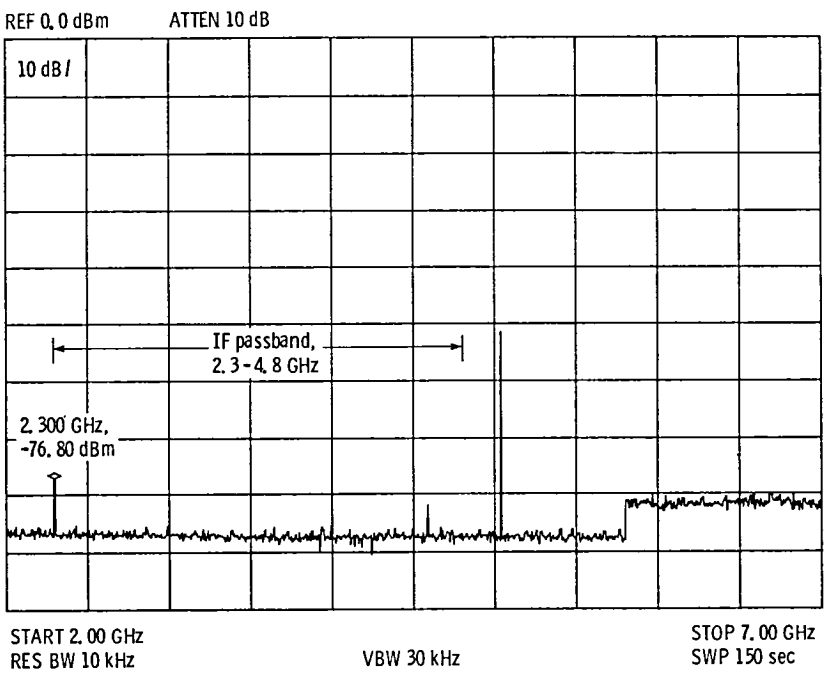

Figure 30. - ITT-2 image rejection test (6/8/83).

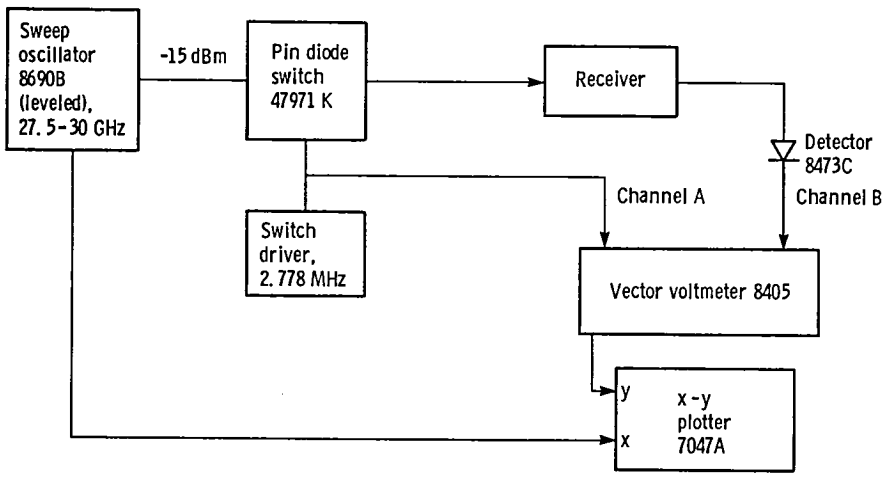

Figure 31. - Block diagram of group delay measurement.

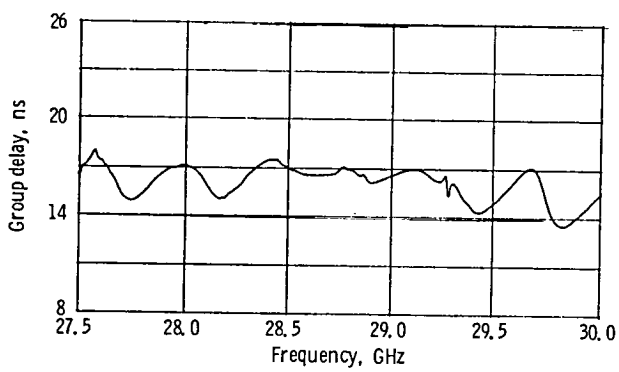

Figure 32. - ITT-1 group delay.

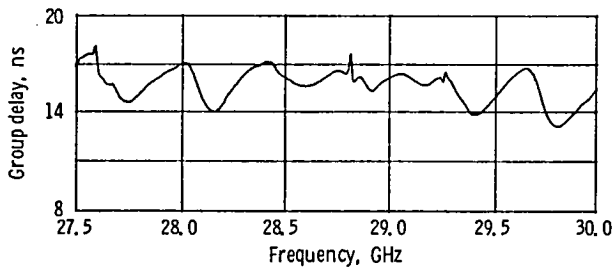

Figure 33. - ITT-2 group delay.

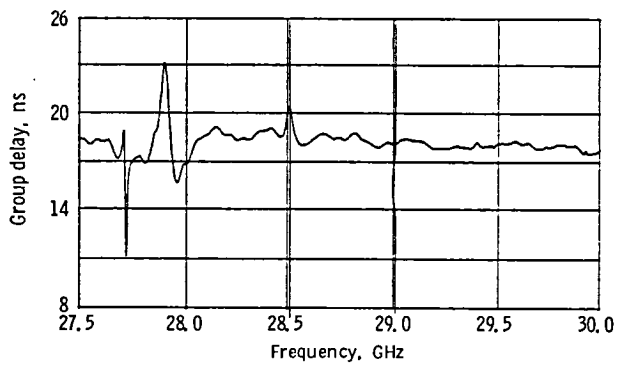

Figure 34. - LNR-1 group delay.

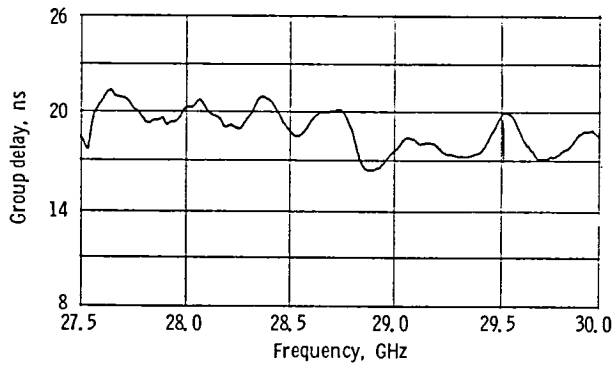

Figure 35. - LNR-2 group delay.

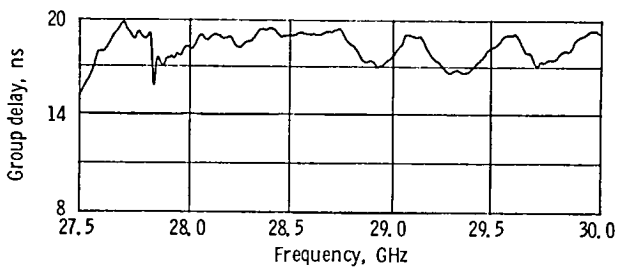

Figure 36. - LNR-3 group delay.

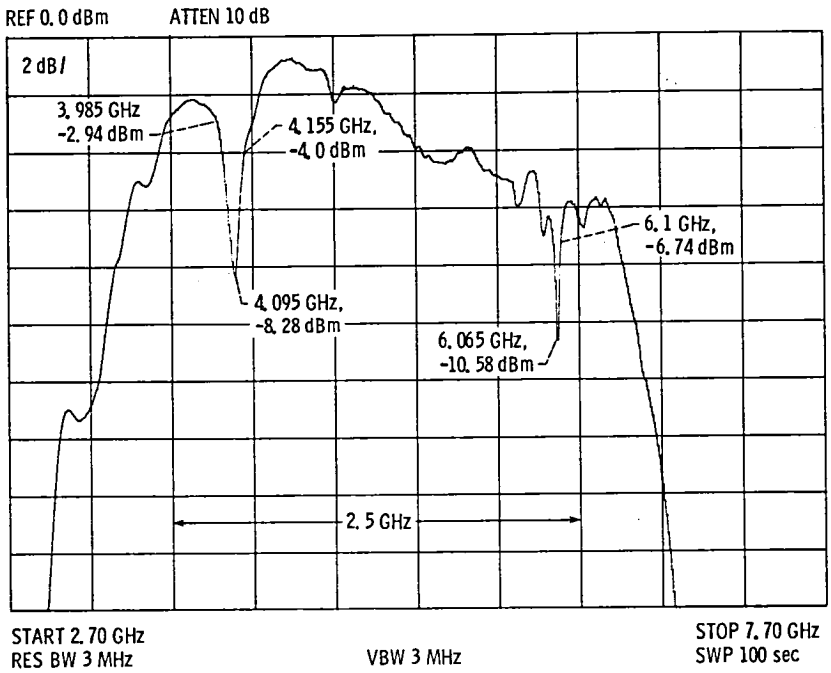

Figure 37. - LNR-1 gain slope test (6/30/83).

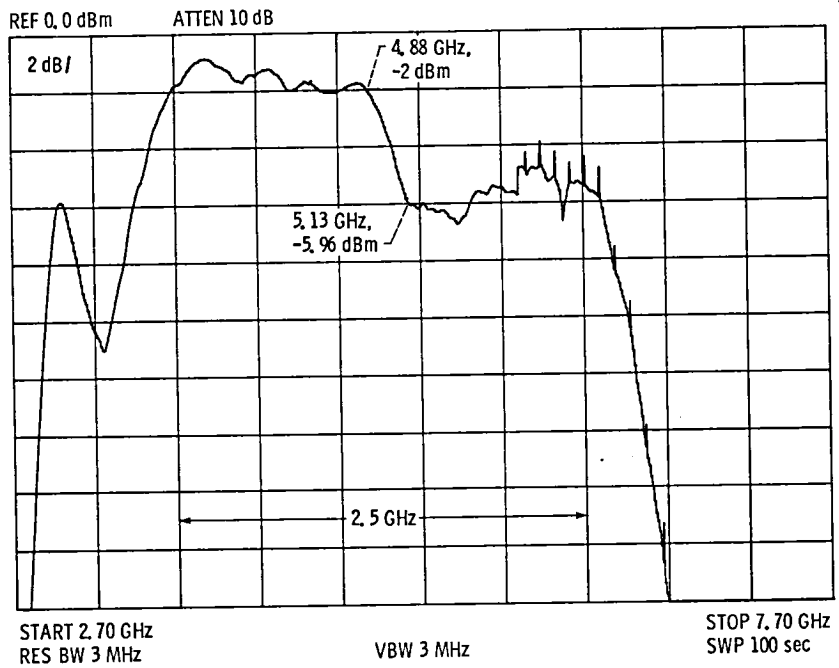

Figure 38. - LNR-2 gain slope test (1/25/83).

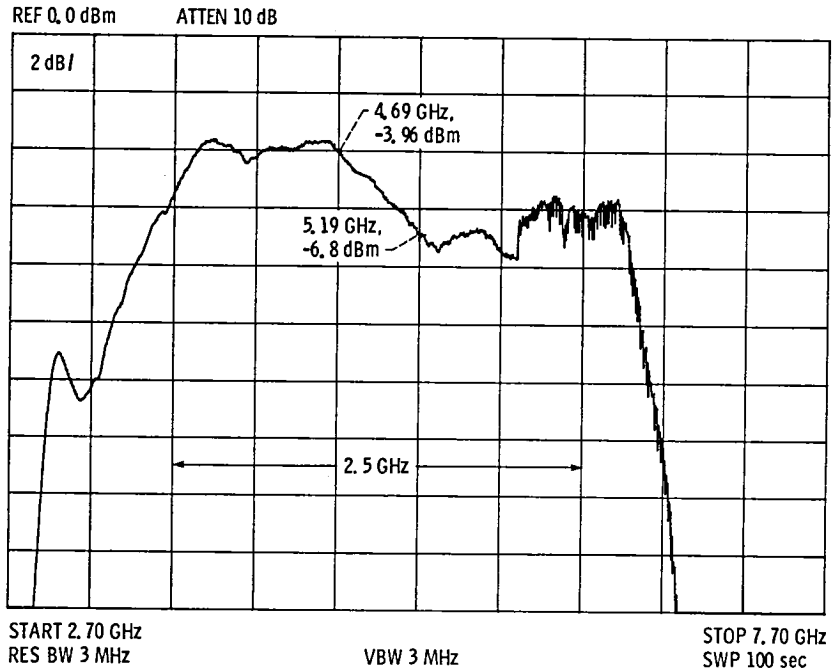

Figure 39. - LNR-3 gain slope test (1/25/83).

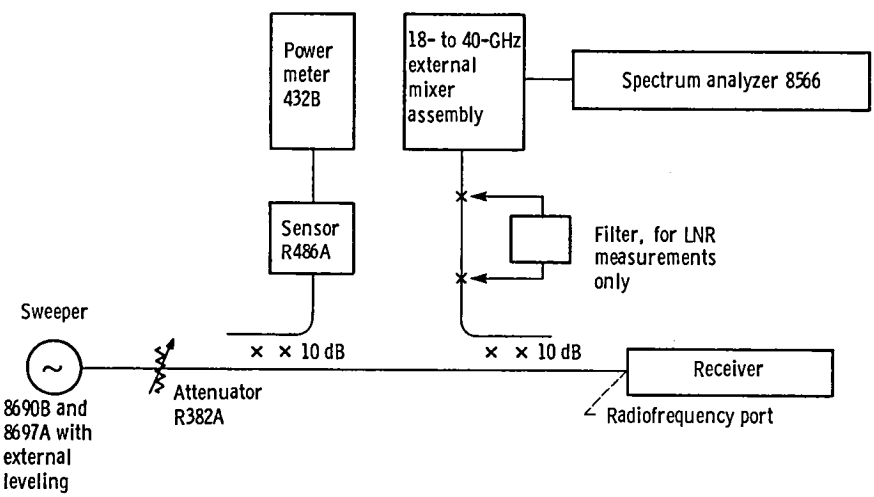

Figure 40. - Block diagram of input voltage standing-wave ratio measurements.

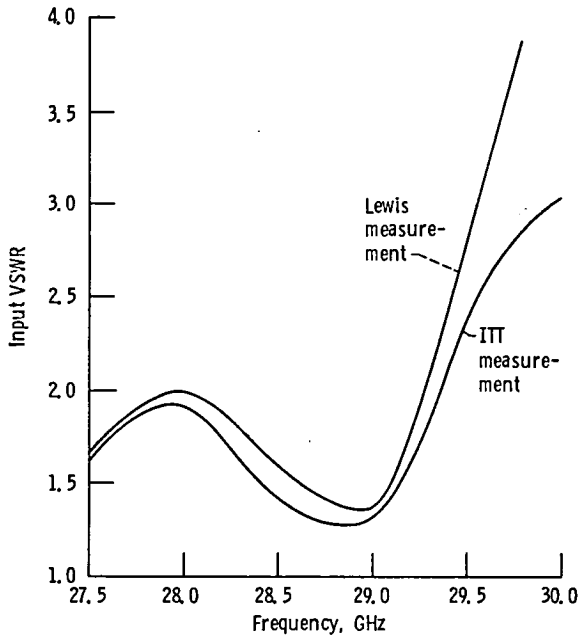

Figure 41. - Input voltage standing-wave ratio versus frequency, ITT receiver 1.

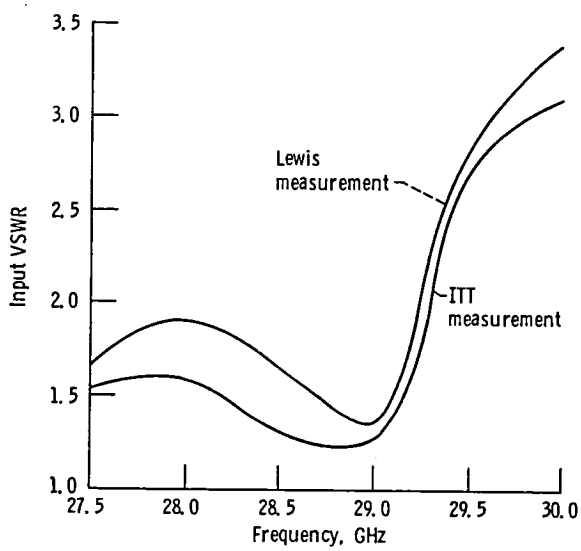

Figure 42. - Input voltage standing-wave ratio versus frequency, ITT receiver 2.

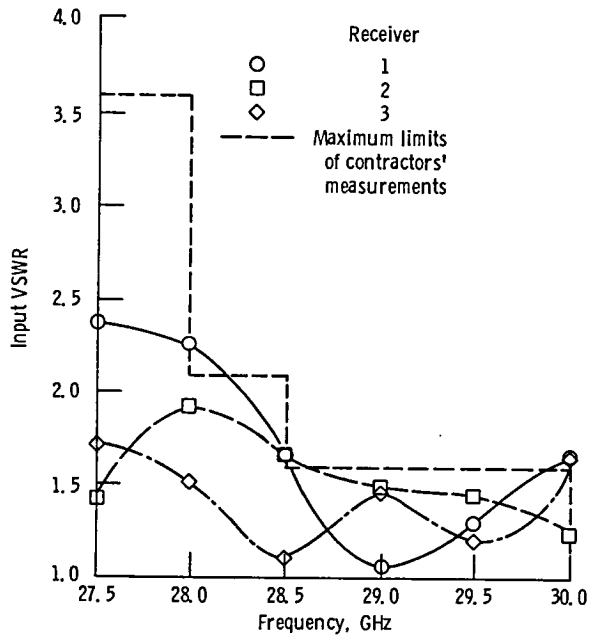

Figure 43. - Voltage standing-wave ratios for LNR receivers.

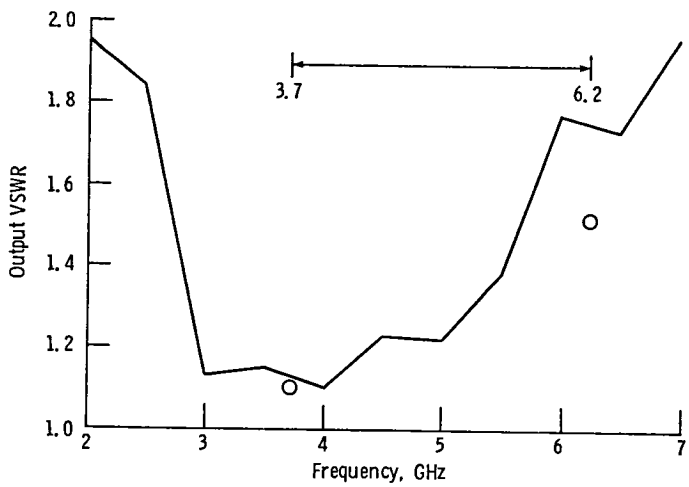

Figure 44. - Output voltage standing-wave ratio versus frequency, LNR receiver 1.

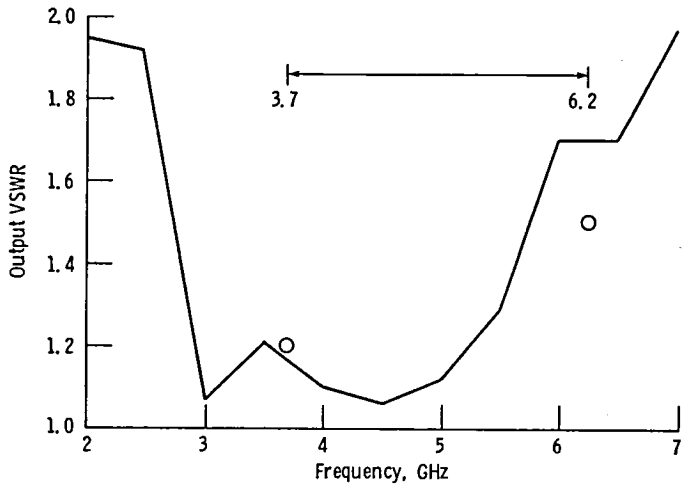

Figure 45. - Output voltage standing-wave ratio versus frequency, LNR receiver 2.

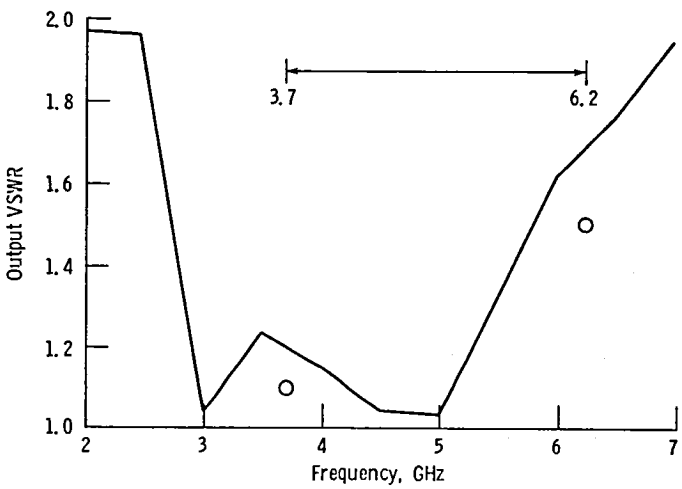

Figure 46. - Output voltage standing-wave ratio versus frequency, LNR receiver 3.

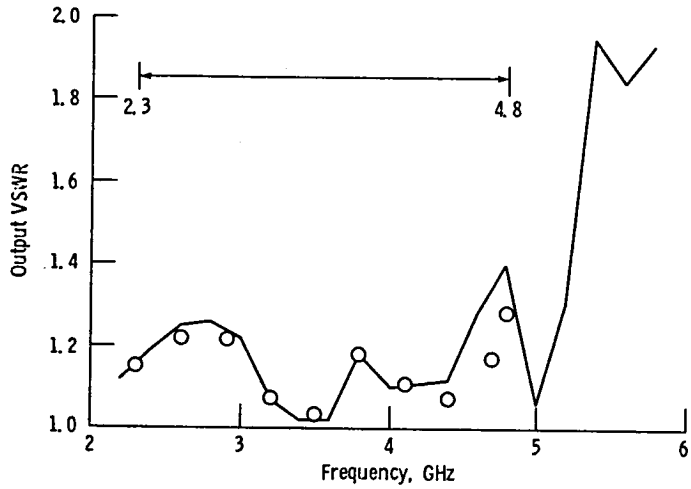

Figure 47. - Output voltage standing-wave ratio, ITT receiver 1.

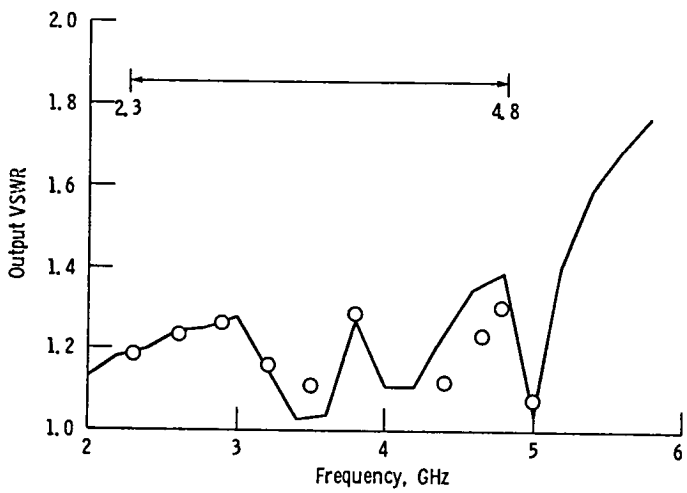

Figure 48. - Output voltage standing-wave ratio, ITT receiver 2.

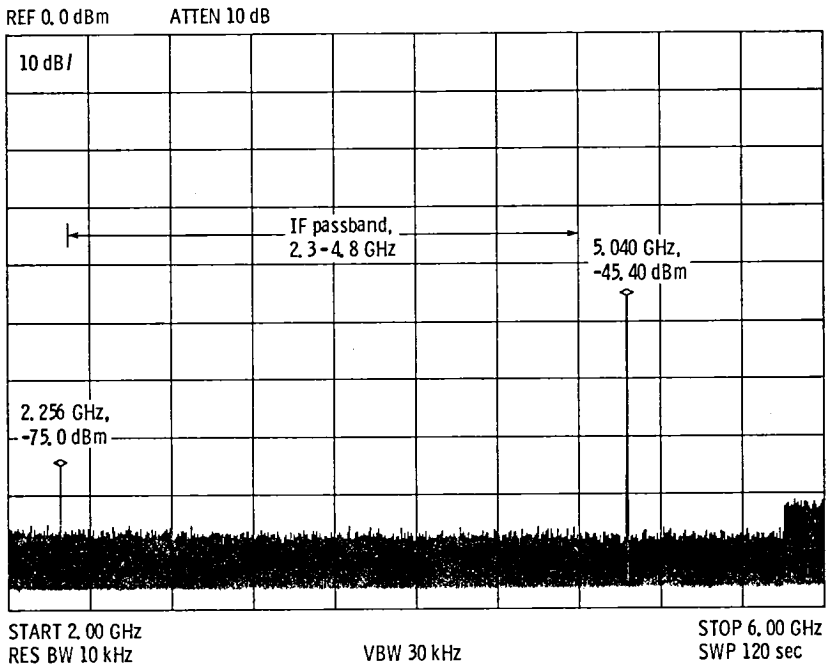

Figure 49. - ITT-1 output spectrum (6/3/83).

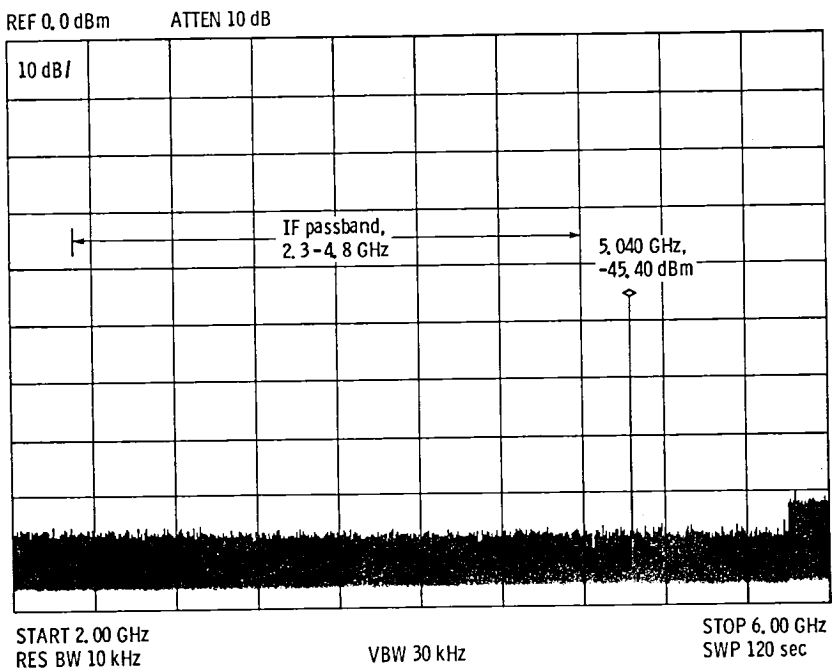

Figure 50. - ITT-2 output spectrum (6/1/83).

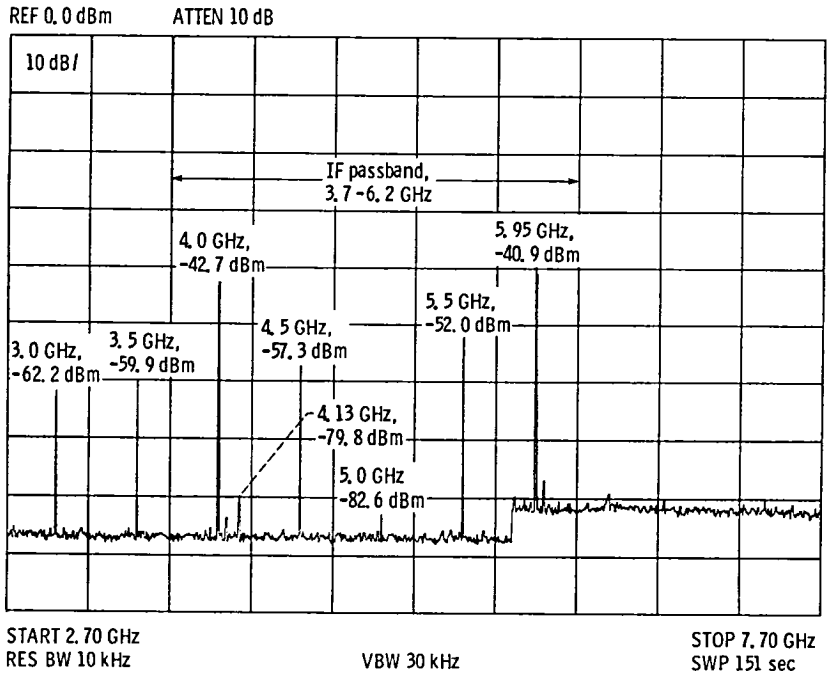

Figure 51. - LNR-1 output spectrum (7/8/83).

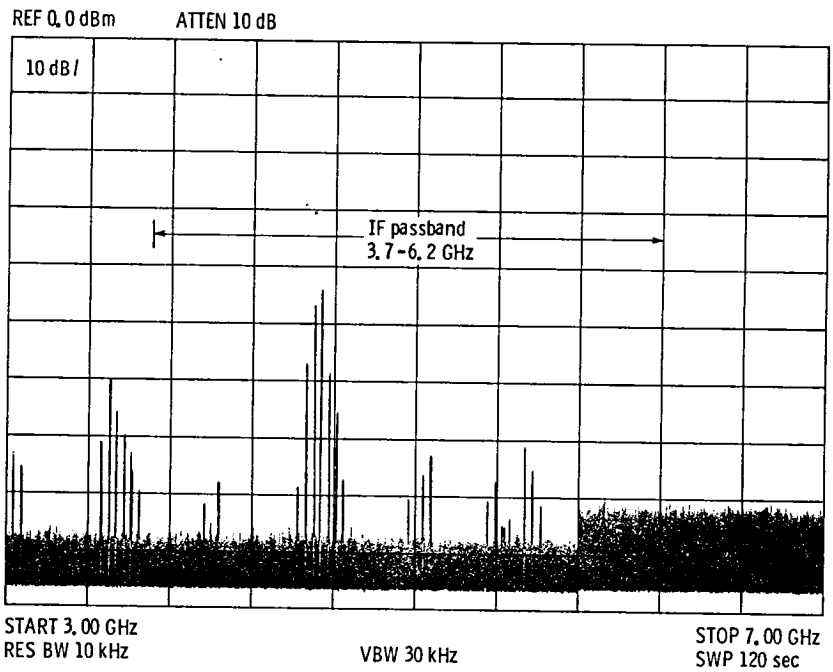

Figure 52. - LNR-2 output spectrum (6/10/83).

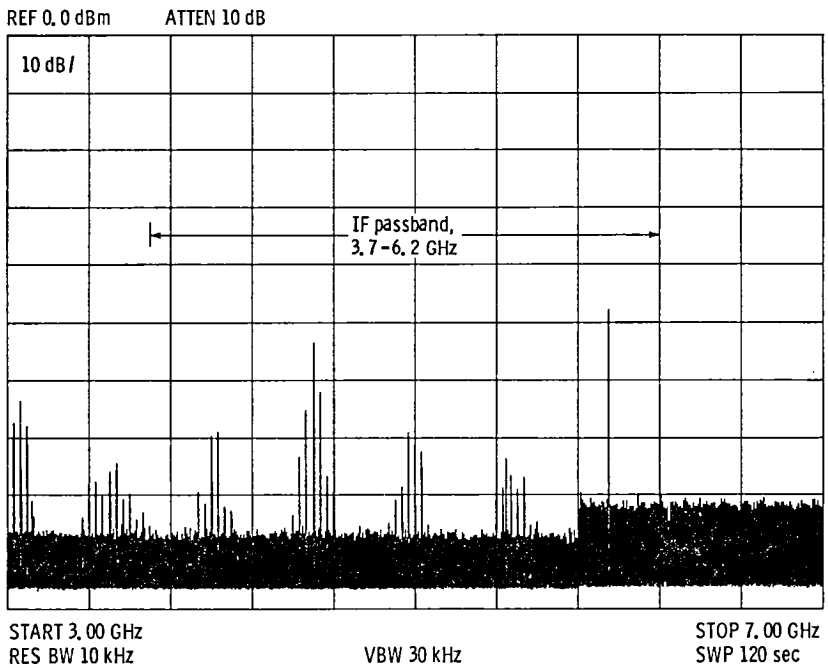

Figure 53. - LNR-3 output spectrum (6/10/83).

1. Report No.	2. Government Accession No.	3. Recipient's Catalog No.
NASA TM-83662		

4. Title and Subtitle	5. Report Date
Test Results for 27.5- to 30-GHz Communications Satellite Receivers	June 1984
	6. Performing Organization Code
7. Author(s)	8. Performing Organization Report No.
Martin J. Conroy	E-1995
	10. Work Unit No.
9. Performing Organization Name and Address	11. Contract or Grant No.
National Aeronautics and Space Administration Lewis Research Center Cleveland, Ohio 44135	13. Type of Report and Period Covered
12. Sponsoring Agency Name and Address	Technical Memorandum
National Aeronautics and Space Administration Washington, D.C. 20546	14. Sponsoring Agency Code

15. Supplementary Notes

16. Abstract

Tests were performed on five proof-of-concept receivers that had been developed by two contractors, LNR Communications, Inc., and ITT Defense Communications, under the NASA 30/20 GHz Technology Development Program. The receivers operate in the 27.5- to 30-GHz uplink band for communications satellites and produce an output at C band. Receiver requirements and test results are given. Test methods are discussed and results are compared with the contractor's test results.

17. Key Words (Suggested by Author(s))	18. Distribution Statement
Communications satellite receivers	Unclassified - unlimited STAR Category 32

19. Security Classif. (of this report)	20. Security Classif. (of this page)	21. No. of pages	22. Price*
Unclassified	Unclassified		

*For sale by the National Technical Information Service, Springfield, Virginia 22161

National Aeronautics and
Space Administration

Washington, D.C.
20546

Official Business
Penalty for Private Use, $300

SPECIAL FOURTH CLASS MAIL
BOOK

Postage and Fees Paid
National Aeronautics and
Space Administration
NASA-451

NASA

POSTMASTER: If Undeliverable (Section 158
Postal Manual) Do Not Return